

Supporting Information

Photophysical Properties of Ligand Localized Excited State in Ruthenium (II) Polypyridyl Complexes: A Combined Effect of Electron Donor-Acceptor Ligand

Sandeep Verma^a, Prasenjit Kar^b, Amitava Das^{b*} and Hirendra Nath Ghosh^{a*}

^a Radiation and Photo Chemistry Division, Bhabha Atomic Research Center, Mumbai, India.

^b Central Salt and Marine Chemicals Research Institute (CSIR), Bhavnagar: 364002, Gujarat, India.

* Correspondence should be addressed to HNG: hngghosh@barc.gov.in, AD: amitava@csmcri.org.

Details of Me₂L₁:

Me₂L₁

Ligand Me₂L₁ was synthesized following a reported procedure.^{23c}

Characterization details of the ligand Me₂L₁:

EI-MS: *m/z* 332 (M⁺, 100%), 317 (M⁺-CH₃, 50%), 302 (M⁺-2CH₃, 28%). ¹H NMR (CD₂Cl₂, ppm): δ 8.6 (1H, d; *J* = 5.2Hz; pyridyl H⁶ or H^{6'}), 8.51-8.55 (2H, m; pyridyl [H⁶ or H^{6'}] and [H³ or H^{3'}]), 8.31 (1H, s; pyridyl H³ or H^{3'}), 7.52 (2H, m; -CH= and pyridyl H⁵ or H^{5'}), 7.1-7.2 (3H, m; pyridyl H⁵ or H^{5'}, phenyl H² and H⁶), 7.1 (1H, d, *J* = 16.3Hz; =CH-), 6.98 (1H, d, *J* = 8.8Hz phenyl H⁵), 3.89 (3H, s; p-OCH₃), 3.85 (3H, s, m-OCH₃), 2.43 (3H, s; CH₃).

Details about the Complex **1Me₂**:

Complex **1Me₂**

Complex **1** was synthesized following the reported procedure.

These complex was synthesised by reaction of [Ru(bpy)₂Cl₂].2H₂O (0.156 gm, 0.3 mmol) with Me₂L₁ (0.120 gm, 0.36 mmol) in ~50 ml ethanol-water mixture at refluxing temperature for 4 hr. Then ethanol was removed under reduced pressure and the complex was precipitated as deep orange solid on addition of excess of aqueous KPF₆ solution. Residue was filtered off, washed with cold water and air-dried. The crude product was purified by gravity chromatography using silica as stationary phase and CH₃CN-saturated aqueous NH₄PF₆ solution (99:1, v/v) as eluent. CH₃CN was removed under vacuo and the pure complex was extracted in CH₂Cl₂ layer. The CH₂Cl₂ layer was dried over anhydrous MgSO₄ and CH₂Cl₂ was removed to isolate the pure compounds **1**. Yields: **1**, 68% (0.259 gm). Elemental analysis: Experimental C 47.4, H 3.43, N

8.07; Calculated for $\text{RuC}_{41}\text{H}_{36}\text{N}_6\text{O}_2\text{P}_2\text{F}_{12}$ is C 47.54, H 3.50, N 8.11; MS (ESI-MS) m/z: 862 ($\text{M}^+ - \text{PF}_6$), 717 ($\text{M}^+ - 2\text{PF}_6$). ^1H NMR (CD_3CN , ppm) for **1**: δ 8.5 – 8.5 (6H, m), 8.07 (4H, t, J = 4.9 Hz), 8.2 - 8.1 (2H, m), 8.08 – 7.81 (4H, m), 7.53 – 7.48 (3H, m), 7.42 – 7.3 (3H, m), 7.15 – 7.05 (3H, m), 6.99 (1H, d, J = 15.8 Hz), 6.8 (1H, d, J = 7.8 Hz), 3.88 (3H, s), 3.84 (3H, s), 2.55 (3H, s). IR (KBr pellet, cm^{-1}) for **1**: 1594 (-C=C- or -C=N-), 1512 (-C=C-, aromatic), 1266 (-C-O), 1023 (-OCH₃), 840 (PF_6).

Details about the Complex **1**:

Complex **1** was synthesized following a standard literature procedure.^{23a,b} Details of the synthetic procedure is provided in the *Review Only Information*. Characterization data for this complex are as follows:

Elemental analysis: Experimental C 46.8, H 3.15, N 8.2; Calculated for $\text{RuC}_{39}\text{H}_{32}\text{N}_6\text{O}_2\text{P}_2\text{F}_{12}$ is C 46.48, H 3.20, N 8.34; MS (ESI-MS) m/z: 862 ($\text{M}^+ - \text{PF}_6$), 717 ($\text{M}^+ - 2\text{PF}_6$). ^1H NMR (CD_3CN , ppm) for **1**: δ 8.55 – 8.47 (6H, m), 8.25 - 8.14 (6H, m), 8.12 – 7.9 (4H, m), 7.6-7.5 (3H, m), 7.42 – 7.3 (3H, m), 7.15 – 7.05 (3H, m), 6.99 (1H, d, J = 15.8 Hz), 6.8 (1H, d, J = 7.8 Hz), 2.55 (3H, s). IR (KBr pellet, cm^{-1}) for **1**: 1596 (-C=C- or -C=N-), 1511 (-C=C-, aromatic), 1264 (-C-O), 837 (PF_6).

a) Effect of pH on electronic transition in Ru^{II}(bpy)₃ complex:

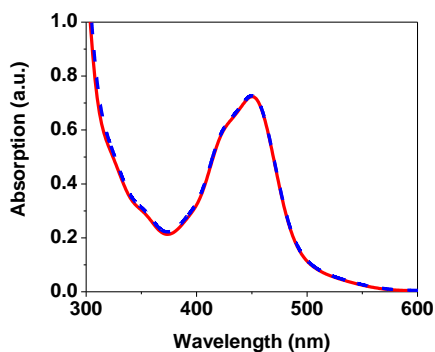


Figure S1- Absorption spectra of Ru^{II}(bpy)₃ in neutral (solid line) and acidic condition (dash line) in acetonitrile solvent.

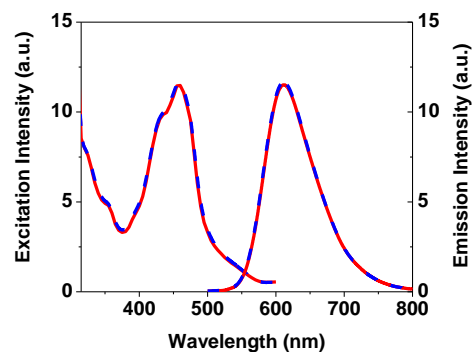


Figure S2: Excitation (at 615nm emission) and emission spectra (at 460nm excitation) of Ru^{II}(bpy)₃ in (a) neutral acetonitrile (solid line) (b) HNO₃-acetonitrile (dash line) solution.

Steady state absorption, excitation and emissions spectra remain same before and after adding HNO₃ (1:100 molar ration) to Ru^{II}(bpy)₃ in acetonitrile solvent.

b) Steady state absorption and emission spectra of L₁ and L₂ molecules (unbound):

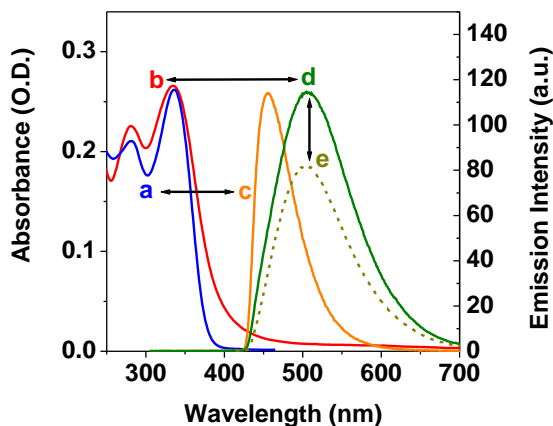


Figure S3: Steady state absorbance spectra of (a) L₁ ligand and (b) L₂ ligand. Emission spectra of (c) L₁ ligand, (d) L₂ ligand with 300nm excitation (bold lines) and (e) L₂ ligand with 400nm excitation (short dash line) in neutral condition in acetonitrile solvent.

Figure-S3 shows steady state absorption and emission spectra of unbound (free) L₁ and L₂ molecules in acetonitrile solvent. The 336 nm peak of L₁ molecule is ascribed to π - π^* (L₁[π] - bpy[π^*]) transitions. The absorption spectra of L₂ molecules extending in 350-550nm region is attributed to intramolecular charge transfer transitions. This is further supported by red shift (~55nm) in emission maxima of L₂ molecules (λ_{em} 455nm) in comparison to that of L₁ molecules (λ_{em} 505nm). Figure -S3d and -S3e shows that emission spectra of L₂ molecules are same at 300 and 400nm excitation wavelength.

c) Effect of pH on 1:1:1 physical mixture of Ru^{II}(bpy)₃, L₁, L₂ molecular species:

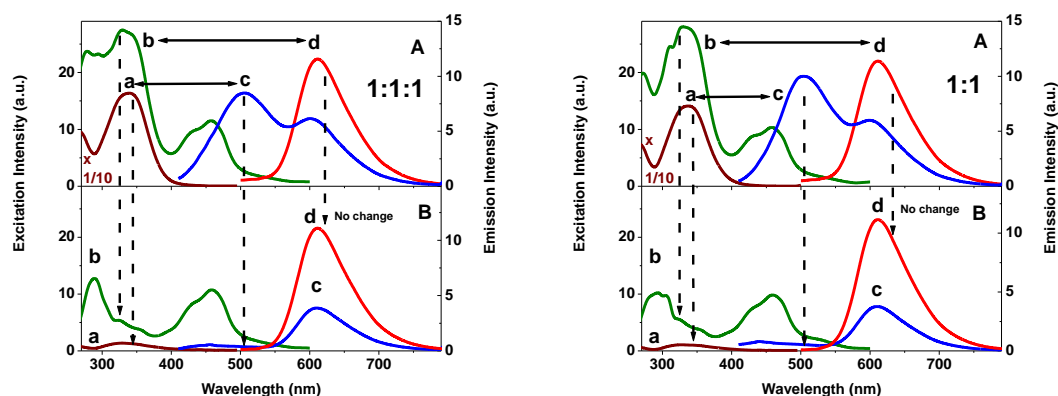


Figure S4: Left Panels - 1:1:1 physical mixture of Ru(bpy)₃ complex, L₁, L₂ ligands ; Right Panels - 1:1 physical mixture of Ru(bpy)₃ complex, L₂ ligand; Top Panels – acetonitrile solvent; bottom panels- HNO₃-acetonitrile solvent. (a) Excitation spectra for 505 emission wavelength (actual intensity divided by 10 in panel-A), (b) excitation spectra for 615 emission wavelength, (c) emission spectra at 400 excitation wavelength and (d) emission spectra at 460nm excitation wavelength

Figure S4 (left panel) shows the protonation effect on excitation and emission spectra of physical mixture (1:1:1) of Ru(bpy)₃ complex, L₁ and L₂ ligands in acetonitrile solvent. The photoexcitation at 400nm exhibit two emission peaks at 505nm and 615nm with a small shoulder at 455nm in neutral condition. However, the 455nm shoulder is not observed in 1:1 physical mixture of Ru(bpy)₃ complex and L₂ ligands as shown in right panel. The observed emission spectra comply with individual contribution of L₁ ligand (455nm), L₂ ligand (505nm) and Ru(bpy)₃ complex (615nm). On protonation, the 505 nm emission peak of L₂ ligand reduces (~14 time) significantly whereas emission due to Ru(bpy)₃ complex at 615nm remain unchanged. In presence of HNO₃, intraligand CT transition are suppressed by protonation of -NMe₂ moiety (electron donor) of L₂ ligand whereas $d\pi_{\text{Ru(II)}} \leftarrow \pi^*_{\text{bpy}}$ MLCT transition (absorption peak at 460nm) in Ru(bpy)₃ complex remains unchanged (figure-S1). Thus, 460nm photoexcitation results identical emission spectra. This is further evidenced in excitation spectra recorded in neutral and acidic conditions. The excitation spectrum for 615nm emission wavelength shows no significant changes in 400-600nm region on protonation. However, the excitation spectra in 300-400nm region are adversely affected with addition of HNO₃ in acetonitrile solution. The excitation spectra in 300-400nm region is dominated by intraligand CT transition of L₂ and $\pi-\pi^*$ of L₁ ligands. Therefore, protonation of -NMe₂ moiety in L₂ ligand causes hypochromic blue shift in excitation peak.

d) LLCT state vs. MLCT state: Steady state excitation and emission spectrum of complex-1 and -3

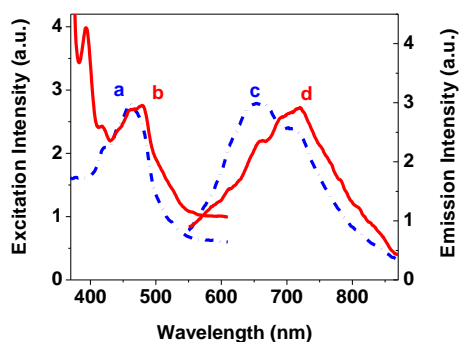


Figure S5- Excitation spectra of complex-3 at a) $\lambda_{\text{emission}} = 640 \text{ nm}$ and b) $\lambda_{\text{emission}} = 720 \text{ nm}$; Emission spectra of complex-2 at c) $\lambda_{\text{excitation}} = 450 \text{ nm}$ and d) $\lambda_{\text{excitation}} = 400 \text{ nm}$. (ethyl acetate solvent).

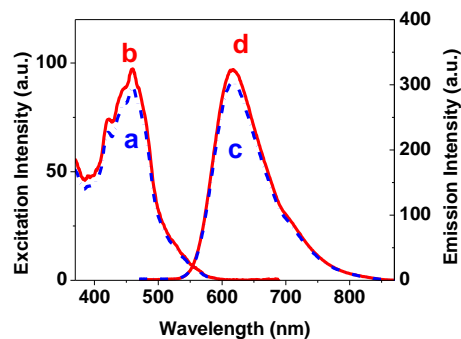


Figure S6: Excitation spectra of complex-1 at a) $\lambda_{\text{emission}} = 620 \text{ nm}$ and b) $\lambda_{\text{emission}} = 715 \text{ nm}$; Emission spectra of complex-1 at c) $\lambda_{\text{excitation}} = 450 \text{ nm}$ and d) $\lambda_{\text{excitation}} = 400 \text{ nm}$.

Figure S5 shows the excitation and emission spectrum of complex-3. Two emission maxima (720nm and 640nm) have been observed after photoexcitation at two different excitation wavelength viz 400nm and 450nm. The 720nm peak corresponds to LLCT state whereas the 640nm peak is attributed to MLCT state. This is supported by photoexcitation spectra monitored for 720nm and 640nm emission wavelength. The excitation spectrum for 720nm emission wavelength shows higher absorbance in 350-425nm and 500-610nm regions as compared to excitation spectra for 640nm emission wavelength. This clearly suggests that LLCT transition dominates in 350-425nm and 500-610nm region whereas the MLCT transition occurs in 425-500nm region. In case of complex-1, no such excitation wavelength dependent emission is observed (Figure S6). This shows that only MLCT excited state exists in complex-1.

Reference: S. Verma, P. Kar, A. Das, H. N. Ghosh, *Chem. Eur. J.*, **2011**, 17, 1561.

e) Optical emission study in deaerated condition:

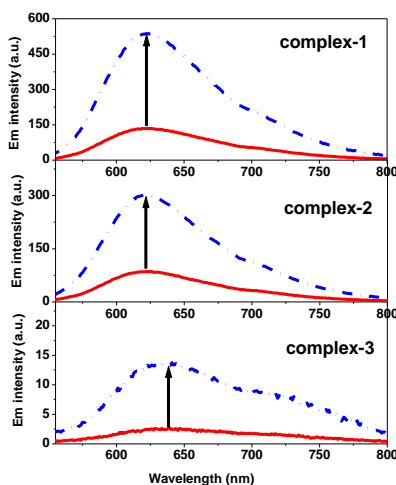


Figure S7- Emission spectra of (a) complex-1, (b) complex-2 and (c) complex-3 in aerated (bold lines) and deaerated (dash-dot lines) condition.

Figure S7 shows the emission spectra of complexes **-1**, **-2** and **-3** in deaerated condition. The deaerated sample is prepared by repeated “freeze-thaw-pump” cycle (five times). In all three cases, an increase in emission intensity was observed in deaerated condition. In aerated condition, due to oxygen quenching, emission from triplet MLCT states of metal-polypyridyl complexes decreases drastically. This oxygen quenching channel has been eliminated by removing trace amount of O₂ dissolved in solution by following five cycle of “freeze-thaw-pump” process. As a result, an increased emission yield is observed in deaerated condition.

f) Nanosecond time resolved emission spectroscopy of complex-1, -2 and -3 in deaerated condition at 300K:

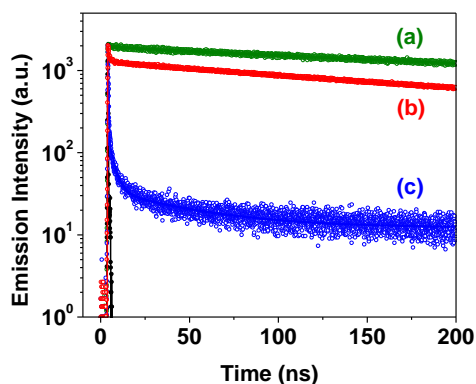


Figure S8- Emission decay kinetics of (a) complex-1, (b) complex-2 and (c) complex-3 at respective emission peak wavelengths in deaerated condition

The emission decay profile of complexes **-1**, **2** and **3** in deaerated condition are shown in figure S8 after exciting the sample at 406 nm wavelength and monitoring the emission at their respective emission peak wavelengths viz 621, 622 and 640nm respectively. The emission decay profile of complex-1 is best fitted bi-exponentially with time constants of 6ns (6%) and 315ns (94%). The short component (6ns) can be attributed to emission lifetime of ³MLCT states associated with bp-CH=CH-cat ligand. The second components (>315ns) is observed with increased life time as compared to aerated condition and resembles to ³MLCT state involving bpy ligand. Shown in Figure-S8b is the emission decay kinetics of complex-2 which is best fitted bi-exponentially with 700ps (45%) and >200ns (55%) time constants. On comparison with emission lifetime of complex-2 in aerated condition we can conclude that the faster component is not due to triplet quenching by O₂, rather it might be intrinsic decay time constant from ³MLCT state to ³ILCT state. Figure-S8c shows the emission decay kinetics of the complex-3 which can be fitted multi-exponentially with time constants of 200ps (95%), 3.2ns (3.2%) and >500ns (1.8%). Here again the shorter component can be attributed to intrinsic decay time constant from ³MLCT state to ³LLCT state.

g) Nanosecond time resolved emission spectroscopy of 1:1:1 physical mixture of Ru^{II}(bpy)₃, L₁ and L₂ molecular species:

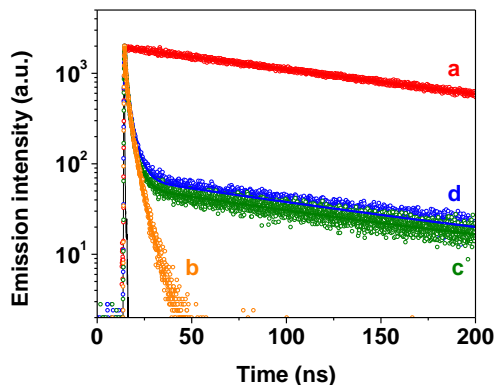


Figure S9- Emission decay kinetics of (a) Ru^{II}(bpy)₃ complex, (b) L₂ molecule, (c) 1:1 physical mixture of Ru^{II}(bpy)₃ and L₂ molecular species (d) 1:1:1 physical mixture of Ru^{II}(bpy)₃, L₁ and L₂ molecular species monitored at 615nm after laser photoexcitation of 406nm.

The Figure-S9 shows the emission decay kinetics of 1:1:1 physical mixture of Ru^{II}(bpy)₃, L₁ and L₂ molecular species in aerated acetonitrile solvent. The 615nm emission kinetics of Ru^{II}(bpy)₃ complex is best fitted with 153 ns time constant and shown in figure-S9a. Figure-S9b shows decay kinetics of L₂ molecule (bpy-ph-NM₂) and best fitted biexponentially with 0.82 ns (77.6%) and 3.56ns (22.6%) time constants. Figure-S9c shows the emission decay kinetics of 1:1 physical mixture of Ru^{II}(bpy)₃ and L₂ molecular species and best fitted tri-exponentially with 0.88ns (72.9%), 3.5ns (24.9%) and 153ns (2.2%). Similar decay profile is observed in 1:1:1 physical mixture of Ru^{II}(bpy)₃, L₁ and L₂ molecular species (figure S9d) which is best fitted with 0.82ns (72.6%), 3.6ns (24.7%) and 153ns (2.7%). In both physical mixtures, the fast decay components (~0.8ns and ~3.5ns) matches well with decay profile of L₂ molecule and can be assigned to emission decay due to free L₂ molecular species. This is also supported by steady state emission measurements where emission yield of 1:1:1 physical mixture is observed to be same as that of pure Ru^{II}(bpy)₃ complex using 455nm photoexcitation (figure-S4 and S2). This suggests that electron or energy transfer process is not occurring in physical mixture of Ru^{II}(bpy)₃, L₁ and L₂ molecular species. So, the fast phase emission quenching (~200ps) observed in complex-**3** corresponds to internal conversion from MLCT excited states to LLCT excited states.

h) Microsecond time resolved emission spectroscopy of complex-1, -2 and -3 at 77K:

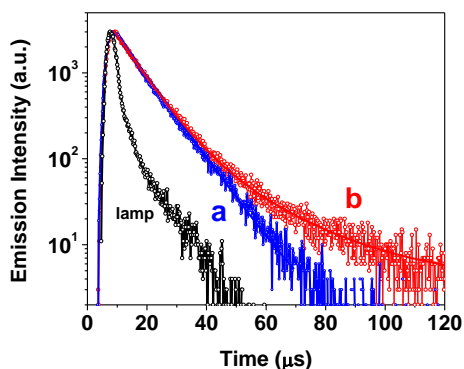


Figure S10- Emission decay kinetics of a) complex-2, b) complex-3 in ethanol/methanol mixture (4:1 v/v) at 77K.

In literature, the emissive life time of ILCT and LLCT states are reported to be in sub-millisecond (ms) time domain whereas the $^3\text{MLCT}$ state lifetime is reported to be in the range of 2-5 microsecond (μs) at 77K. Since, the excitation lamp profile in the present setup is too broad (FWHM \sim 3-4 μs , Figure-S10 lamp) to measure $^3\text{MLCT}$ decay kinetics of complex-1. So, only the emission decay kinetics of complex-2 (Figure-S10a) and complex-3 (Figure-S10b) are presented here. The luminescent decay kinetics of complex-2 can be fitted single exponentially with time constant of 9 μs (Figure-S10a). However, the emission decay kinetics of complex-3 (Figure- 10b) can be fitted biexponentially with time constants of 9 μs and 22 μs . Here the long component (22 μs) is attributed to $^3\text{LLCT}$ state of complex-3.